Hydrochemical Characteristics and Quality Assessment of Shallow Groundwater in Yangtze River Delta of Eastern China

Taotao Lu
Bayreuth University: Universitat Bayreuth
Runzhe Li
Shandong Agricultural University
Aira Sacha Nadine Ferrer
Bayreuth University: Universitat Bayreuth
Shuang Xiong
Wuhan Zondy W&R Environmental Technology Co.
Pengfei Zou
Yantai New Era Health Industry Chemical Co.
Hao Peng (penghao@cug.edu.cn)
China University of Geosciences

Research Article

Keywords: Yangtze River Delta, Hydrochemistry, Shallow groundwater quality, Health risk assessment

Posted Date: October 18th, 2021

DOI: https://doi.org/10.21203/rs.3.rs-931598/v1

Version of Record: A version of this preprint was published at Environmental Science and Pollution Research on March 28th, 2022. See the published version at https://doi.org/10.1007/s11356-022-19881-w.

Hydrochemical characteristics and quality assessment of shallow groundwater in Yangtze River Delta of eastern China

Taotao Lu [1, 5], Runzhe Li [2], Aira Sacha Nadine Ferrer [1], Shuang Xiong [3],

Pengfei Zou [4], Hao Peng [5, *]

[1] Department of Hydrology, Bayreuth Center of Ecology and Environmental Research (BAYCEER), University of Bayreuth, Bayreuth, 95440, Germany

[2] Faculty of Public Administration, Shandong Agriculture University, Taian, 271011, China

[3] Wuhan Zondy W&R Environmental Technology Co., Ltd, Wuhan, 430078, China

[4] Yantai New Era Health Industry Chemical Commodity Co., Ltd., Yantai 264000, China

[5] School of Environmental Studies, China University of Geoscience, Wuhan, 430078, China

Manuscript prepared for *Environmental Science and Pollution Research*

*Corresponding author: Hao Peng (penghao@cug.edu.cn; Tel. +86 (0)27-87057085)

Abstract

The water resource is highly demanded in the Yangtze River Delta with a developed economy. Long-term exploitation has posed threats of artificial pollution and seawater intrusion to the shallow groundwater. This study aimed to reveal the hydrochemical characteristics and health risks of shallow groundwater in the coastal plain of the Yangtze River Delta. Also, possible factors affecting groundwater quality were discussed. Methods, such as typical hydrochemical tests, water quality assessment and health risk models, were applied to achieve the study targets. The results showed that the shallow groundwater was slightly alkaline, and the average values of total dissolved solids (TDS) and total hardness (TH) were 930.74 mg/L and 436.20 mg/L, respectively. The main hydrochemical types of groundwater were Ca+Mg–HCO_3 and Ca/Na–HCO_3, accounting for 44.3% and 47.5%, respectively. In addition, As concentration was generally high, with a mean value of 0.0115 mg/L. The principal factors affecting the groundwater components include water-rock interactions (especially silicate), cation exchange, seawater intrusion and human activities. As in the groundwater is strongly influenced by the redox of Fe, Mn, and NO_3^-. The results of the groundwater quality evaluation indicated that the shallow groundwater in some regions was unsuitable for drinking and agricultural irrigation. Health risk assessment showed that 44.3% of the water samples had significant health risks, which was attributed to the high As concentration. Therefore, it is urgent to establish long-term As monitoring to maintain sustainable groundwater management and drinking water safety. The

results of this study can provide essential data for water resource management and human health protection in the Yangtze River Delta.

Keywords: Yangtze River Delta; Hydrochemistry; Shallow groundwater quality; Health risk assessment

1. Introduction

Shallow groundwater is a crucial water source for industrial and agricultural production as well as daily life due to its shallow buried depth and easy accessibility (Li et al. 2020; Liu et al. 2021d). The shallow groundwater quality plays a critical role in urban development and resident health. However, a growing number of studies have proposed that shallow groundwater in many places became unsuitable for drinking and production resulting from the impact of the natural environment and human activities (Hao et al. 2020; Lima et al. 2020). Water salinization and the enrichment of some harmful trace elements, like As, F, etc., in shallow groundwater pose a danger to both ecological safety and physical health (Liu et al. 2021d; Long et al. 2021; Wang et al. 2020; Wu and Sun 2016). In recent years, groundwater quality and health risk assessment have become an essential part of research on medical geology (Selinus et al. 2016). The distributions, sources, and contamination levels of inorganic components in shallow groundwater are the foundation for pollution evaluation and management.

The evolution of shallow groundwater in estuary and delta areas is quite complex. Due to

58 the influence of weather, depositional environment, and anthropological activities, the shallow
59 groundwater environment is fragile (Zhi et al. 2021). Cao et al. (2020) found that the
60 groundwater salinization and nitrate contamination in estuary and delta areas in Qinhuangdao
61 city in northern China were caused by seawater infiltration and agricultural pollution. Hou et al.
62 (2020) proposed that the discharge of domestic and industrial wastewater during urban
63 development had led to increased Mn concentration in shallow groundwater in the Pearl River
64 Delta plain. More and more studies have revealed growing deterioration of shallow groundwater
65 quality in estuary and delta areas (Li et al. 2018). These studies analyzed the hydrogeochemical
66 features and the evolution of groundwater quality. Still, less attention has been paid to the impact
67 of groundwater quality on human health.
68 The Yangtze River Delta plain is one of the fastest growing urban areas with the most
69 developed economy in China. Groundwater exploitation is increasing year by year as a result of
70 rapid population growth. Due to its unique geographical and geological environment, previous
71 studies mainly focused on ground subsidence caused by groundwater extraction (Ma et al. 2018).
72 Even though the Yangtze River Delta plain has abundant groundwater resources, human
73 activities have led to a remarkable deterioration in water quality (Wu et al. 2014). In addition, the
74 groundwater buried depth is relatively small in this area; thus, high TDS in groundwater is found
75 due to the intense evaporation, and the value of TDS is on an upward trend, even tending towards
76 salinization (Zhao et al. 2017). Meanwhile, the research on the variation of shallow groundwater

77 quality in the Yangtze River Delta coastal plain proposed that seawater intrusion contributed to
78 groundwater salinization and exerted a substantial influence on groundwater quality according to
79 the analysis of Sr, O, and H isotopes in groundwater (Mao et al. 2020). Although the
80 deterioration of water quality in the Yangtze River Delta has attracted much attention, there are
81 still no studies on shallow groundwater quality and health risks. In particular, thus far, the spatial
82 distributions and sources of trace elements, groundwater quality and related controlling factors
83 are unknown in the Yangtze River Delta plain.

84 Based on these considerations, shallow groundwater samples were taken from the coastal
85 plain in the Yangtze River Delta; then the dissolved inorganic ingredients in the groundwater
86 were systematically analyzed to achieve the following targets: (1) identify the hydrochemical
87 characteristics of shallow groundwater in this area; (2) evaluate shallow groundwater quality and
88 possible impacts on physical health. These findings can provide valuable information for water
89 resource management and physical health protection in the Yangtze River Delta.
90

91 **2. Materials and methods**

92 *2.1. Study area description*

93 The study area, located in Jiangsu province, China, is flanked by the Yellow Sea to the east
94 and the Yangtze River to the south. It is a typical estuarine delta plain. The topography of this
95 area is, in general, flat and the altitude decreases from west to east. The regional climate is the
96 humid subtropical monsoon climate with average annual precipitation and evaporation of 1050.8

97 mm and 877.2 mm, respectively.

98 The shallow aquifers in the study area consist of the Quaternary Holocene estuarine and
99 coastal unconfined aquifer groups. The porous media is constituted by gray, gray-green silt and
100 silty sub-sandy loam. The lower bedding layer is comprised of shallow marine silty sub-clay
101 deposits, and its bottom slab is buried at a depth of about 30 m with an average thickness of 27
102 m. The aquifers change from unconfined aquifers to slightly confined aquifers towards the east;
103 simultaneously, the groundwater quality gradually becomes saline (Mao et al. 2020). The
104 primary recharge sources of shallow groundwater are atmospheric precipitation and inflow of the
105 Yangtze River and its branches. Since the terrain is relatively flat, the groundwater flow in
106 aquifers is sluggish under the control of topography. Groundwater discharge mainly includes
107 near-surface evaporation and artificial exploitation. Overall, in the research area, the water
108 quality of shallow groundwater is quite complicated because the groundwater was salinized by
109 Holocene marine intrusion and then gradually desalinated by the large quantity of fresh water
110 from the Yangtze River and atmospheric precipitation. In addition, the Yangtze River Delta is one
111 of the most densely inhabited regions in China. Seawater intrusion resulting from a large amount
112 of groundwater extraction and industrial and agricultural pollution have caused a non-negligible
113 impact on the shallow groundwater in this area (Zhao et al. 2017).

114

115 *2.2 Groundwater sample collection and measurement*

In this study, 61 water samples, all of which were shallow groundwater, were taken from the domestic wells in the study area in August 2019. The depth of these wells was less than 10 m. Meanwhile, 1 seawater sample was obtained from the sea near the study area, and 1 rainwater sample was taken in the middle of the study area (see Fig 1). The specific sampling procedure based on our previous studies (Peng et al. 2021a; Peng et al. 2021b) could be found in the supplementary material. The concentrations of trace elements and major elements in the water samples were obtained through ion chromatography, the inductively coupled plasma emission mass spectrometer and standard HCl titration. The measurement process was provided in the supplementary material. In addition, some parameters like pH and TDS were measured on-site by a portable analyzer.

The statistical analysis of obtained data was carried out by SPSS software (IBM 23). During the correlation analysis of each component in groundwater, in the first place, to determine whether the data conform to a normal distribution, the Kolmogorov-Smirnov (K-S) test and Shapiro-wilk test were applied separately. However, the hydrochemical indicators except for pH were not in accordance with the normal distribution; thereby, the Spearman model was adopted for correlation analysis. At last, the spatial distribution of hydrochemical indicators was drawn by ArcGIS software (version 10.5) according to the inverse distance weighting interpolation.

2.3 Groundwater quality assessment

135 *2.3.1 Groundwater quality assessment for agricultural irrigation*

136 Sodium adsorption ratio (SAR) and sodium percentage (Na %), which can be calculated by

137 the equations (Eqs.) (1–2), are usually used to estimate whether groundwater is suitable for

138 irrigation (Long and Luo 2020). Na plays a vital role in irrigation water classification because of

139 its interaction with the soil. Na with a high concentration in irrigation water is readily adsorbed

140 on clay minerals in the soil, replacing Mg and Ca. Besides, the ion exchange of Na with Mg and

141 Ca reduces soil permeability. SAR is considered to be an essential indicator for the evaluation of

142 irrigation water quality. When this indicator is high, the groundwater is not suitable for irrigation.

143 $$\mathrm{Na\%}=\left(\frac{\mathrm{Na+K}}{\mathrm{Ca+Mg+Na+K}}\right)\times 100\% \quad (1)$$

144 $$\mathrm{SAR}=\frac{\mathrm{Na}}{\sqrt{\frac{\mathrm{Ca+Mg}}{2}}} \quad (2)$$

145

146 *2.3.2 Groundwater quality assessment for drinking purpose*

147 The water quality index (WQI) is widely used for drinking water quality assessment since

148 Horton proposed it in the 1960s. The critical point of WQI calculation is to determine the weight

149 of each water quality indicator because minor changes in weight will change the assessment

150 result (Zhang et al. 2020). The methods that are commonly used to determine the weight are the

151 objective weighting method (e.g., entropy-weighted method and criteria importance though inter-

152 criteria correlation method) (Zhang et al. 2021) and the subjective weighting method (e.g., order

153 relation analysis method) (Gao et al. 2020). The subjective weighting method is based on the

154 investigator's actual experience, which brings multiple uncertainties to the result due to the
155 different preferences of different investigators (Islam et al. 2020). Although the objective
156 weighting method does not rely on subjective judgment and has a solid mathematical basis, it
157 fails to reflect the degrees of importance of different indicators to the decision-maker
158 (Narayanamoorthy et al. 2020). Therefore, this study used the integrated-weight method, which
159 combines the subjective and objective weighting methods.

160 In the subjective weighting part, the weighting value (w_{j1}) of the water quality indicator is
161 determined by its relative perceived effect and importance on human health, which can be
162 calculated by the following Eq.(3).

163 $$w_{j1}=\frac{P_j}{\sum P_j} \quad (3)$$

164 Where P_j is the importance score of water quality indicator j, which varies in the range of 1–5 (1
165 shows the minimal impact on water quality; 5 indicates the most significant impact on water
166 quality), for example, heavy metals, such as As, Cd, Cr, and Pb, are harmful to physical health,
167 so their *P* values are 5. The importance score of the different hydrochemical indicators can be
168 found in Table S1.

169 In the objective weighting part, the weight of water quality indicator j (w_{j2}) is determined
170 using the entropy weight method. The specific procedures are as follows:
171 In the first place, the initial data are standardized to obtain initial matrix X (Eq.(4)).

$$X=\begin{bmatrix} x_{11} & \cdots & x_{1n} \\ \vdots & \ddots & \vdots \\ x_{m1} & \cdots & x_{mn} \end{bmatrix} \quad (4)$$

Where m is the total number of groundwater samples; n is the total number of measured hydrochemical indicators in one sample.

After that, the initial matrix X is reversely normalized with Eq. (5) to get the standard matrix Y (Eq.(6)).

$$y_{ij}=\frac{(x_{ij})_{max}-x_{ij}}{(x_{ij})_{max}-(x_{ij})_{min}} \quad (5)$$

$$Y=\begin{bmatrix} y_{11} & \cdots & y_{1n} \\ \vdots & \ddots & \vdots \\ y_{m1} & \cdots & y_{mn} \end{bmatrix} \quad (6)$$

At last, the w_{j2} are obtained by Eqs. (7–9) (Islam et al., 2020):

$$y_j=\frac{y_{ij}+10^{-4}}{\sum_{j=1}^{m}(y_{ij}+10^{-4})} \quad (7)$$

$$e_j=-\frac{1}{\ln m}\sum_{i=1}^{m} y_j \ln y_j \quad (8)$$

$$w_{j2}=\frac{1-e_j}{\sum_{j=1}^{n}(1-e_j)} \quad (9)$$

Based on the Eqs. (3 and 9), the integrated weight can be calculated by following Eq.

$$W_j=\frac{w_{j1}\times w_{j2}}{\sum_{j=1}^{n} w_{j1}\times w_{j2}} \quad (10)$$

After calculating the weights (w_{j1}, w_{j2}, and W_j values are provided in Table S1), the WQI value is calculated by Eq. (11) (see Table S2).

$$WQI=\sum_{j=1}^{n}[W_j\times(\frac{C_j}{S_j})\times 100] \quad (11)$$

where C_j is the value of water quality indicator j in the water sample; S_j is the upper limit of the water quality indicator j in the national standard for drinking water quality (GB 5749-2006). The groundwater can be classified into five categories based on the calculated WQI value: (1) excellent (WQI < 25); (2) good (25 < WQI < 50); (3) medium (50 < WQI < 100); (4) poor (100 < WQI < 150) and (5) extremely poor (WQI > 150).

Hazard Index (HI) is the most commonly used method to evaluate the risk of trace elements in groundwater to human health. Because children are the most sensitive to the exposed heavy metals, the analysis in this study focused on the children's HI (Chen et al. 2020). There are two main exposure pathways to the contaminants in drinking water: dermal absorption (e.g., bathing) and oral ingestion (e.g., drinking water). Therefore, the health risk evaluation of components in groundwater was estimated based on these two main pathways in this research. The specific equations to calculate the HI value can be found in the supplementary material. Table S2 presented the calculated HI values. Overall, when HI is less than 1, there is no health hazard. Even if a health hazard is produced, it is negligible and difficult to be detected. In contrast, HI > 1 means an adverse effect on health.

3. Results and discussion

3.1 Hydrochemical features of shallow groundwater in the study area

The statistical characteristics of the main components in shallow groundwater in the study

207 area are shown in Table 1. The pH of the groundwater samples varied between 6.90 and 7.90,
208 with a mean of 7.31, indicating that the groundwater in the study area is slightly alkaline. The
209 TDS fell in the range of 411.45 – 2361.77 mg/L, with an average of 930.74 mg/L. 67.21% of the
210 groundwater samples were freshwater (TDS <1000 mg/L). The TH ($CaCO_3$) was in the range of
211 181.63 – 897.74 mg/L, and the mean TH was 436.20 mg/L. Based on the TDS and TH values,
212 the groundwater in the study area fell into moderately hard, hard, and very hard water (see Fig.
213 S1(a)). From Fig. S2, it could be found that the contents of major cations followed the order of
214 Na > Ca > Mg > K, with mean values of 124.08 mg/L, 87.46 mg/L, 52.21 mg/L, and 22.80
215 mg/L, respectively. Among them, the maximum Na content was 482.79 mg/L, which exceeded
216 its upper limit (250 mg/L) in the national drinking water quality standard (GB5749-2006).
217 Similarly, the contents of main anions followed the sequence of HCO_3^- > Cl^- > SO_4^{2-} > NO_3^-,
218 with average values of 543.87 mg/L, 117.99 mg/L, 96.12 mg/L and 32.29 mg/L, respectively.
219 The maximum values of Cl^-, SO_4^{2-} and NO_3^- contents were 806.00 mg/L, 271.90 mg/ L, and
220 139.77 mg/L, all of which exceeded the upper limits in the drinking water standard (GB5749-
221 2006). In addition, the Piper diagrams indicated that the shallow groundwater in the study area
222 had four different types (see Fig. S1(b)). The main types were Ca+Mg – HCO_3 and Ca/Na –
223 HCO_3, accounting for 44.3% and 47.5%, respectively, while the remaining ones were Na – HCO_3
224 and Na – Cl.
225 By analyzing the spatial distribution of hydrochemical indicators, the features of

226 groundwater hydrochemistry can be more clearly understood in the study area. As indicated in
227 Fig. 2(a), the TDS values of shallow groundwater ranged from 400 mg/L to 1000 mg/L; and the
228 groundwater samples with high TDS were distributed in the middle part of the study area and
229 coastal regions. In terms of TH (see Fig. 2(b)), groundwater with relatively high TH was located
230 in the west part of the study area, such as Rugao city and Nantong city; In contrast, the
231 groundwater in the east part had low TH. The spatial distributions of Na and Cl^- were similar, as
232 shown in Fig. 2(c, d), with the highest concentrations in the middle part of the study area and
233 coastal regions, while their concentrations were low in the west. The spatial distribution of SO_4^{2-}
234 was different from that of Na and Cl^-, with relatively high levels in the west and relatively low
235 levels in the east (see Fig. 2(e)). The spatial distribution of NO_3^- varied irregularly; the relatively
236 high NO_3^- levels were found in the agricultural regions of Rugao city, Haimen city, and Qidong
237 city (see Fig. 2(f)).

238 The statistical characteristics of trace elements in shallow groundwater can be found in
239 Table 1 and Fig. S2(b). The average concentrations of trace elements followed the below order:
240 Sr > Br > F^- > B > 0.1 mg/L > Ba > Al > Fe > Zn > Mn > Li > As > 0.01 mg/L > Cu > Se > Cr =
241 Ni > Mo > 0.001 mg/L > Others (Co, Ag, Cd, Sn, Sb, W, Tl, Pb and Be). Sr, Br, F^- and B were
242 the main trace elements and their average values (maximum values) were 0.4975 mg/L (0.9882
243 mg/L), 0.3729 mg/L (2.6350 mg/L), 0.3470 mg/L (1.0790 mg/L) and 0.2888 mg/L (1.0065
244 mg/L), respectively. It is also worth noting that the maximum values of F^-, B, Al, Fe, Mn, As, Se,

245 Cr and Ni exceeded the upper limit in the drinking water standard (GB5749-2006).

246 The spatial distributions of typical trace elements are illustrated in Fig. 3. The groundwater
247 samples from coastal regions contained higher F^- levels than non-coastal regions in the study
248 area. Similarly, the groundwater samples with higher B content were distributed in the coastal
249 regions; the highest B content was found in the western part of Haimen city. The groundwater
250 samples containing the highest Al, Fe, and Ni concentrations were from the central and
251 southeastern regions. In addition, groundwater having the highest Mn level was found in Rugao
252 city. The As level in shallow groundwater was generally high; in particular, Nantong city and the
253 southeastern part of Qidong city had higher As concentrations than other regions. Except for one
254 water sample from the north of Qidong city containing high Se levels, the Se concentrations in
255 the rest regions were below 0.002 mg/L.

256

257 *3.2 Shallow groundwater genesis and pollution sources in the study area*

258 In order to obtain the shallow groundwater genesis, the ratios of different components in
259 groundwater were calculated and analyzed. Gibbs diagram can reflect the degree of influence of
260 evaporation,water-rock interaction, and precipitation on the evolution of groundwater
261 hydrochemistry (Gibbs 1970). In this study, most groundwater samples were found in the rock
262 dominance and evaporation zones (see Fig. S3), which means groundwater hydrochemistry is
263 mainly influenced by rock weathering. At the same time, evaporation and concentration also play

264 a crucial role in groundwater quality (Samsudin et al. 2008).

265 Carbonate rock, silicate rock, and evaporite rock are the primary weathered materials, and
266 different rocks will lead to varying levels of ions in the groundwater after weathering. As shown
267 in Fig. S4(a, b), the water-rock interaction in the study area was largely controlled by the
268 weathering of silicate rocks. In addition, the ratio of $(Ca+Mg)/(HCO_3^-+SO_4^{2-})$ could denote the
269 effect of dissolution of carbonate rocks and gypsum on the water quality (Liu et al. 2021c).
270 According to Fig. S4(c), some points fell on the 1:1 line, suggesting that the dissolution of
271 carbonate rocks and gypsum also contributed to the evolution of groundwater quality. As
272 illustrated in Fig. S4(d), Ca and Mg in most groundwater samples derived from the dissolution of
273 dolomite and calcite (Argamasilla et al. 2017). Furthermore, most groundwater samples had
274 Na/Cl^- ratios close to the seawater-freshwater mixing line in Fig. 4(a), indicating that the main
275 source of Na and Cl^- is seawater intrusion. For the purpose of further evaluating the extent of
276 seawater intrusion, seawater fraction (f_{sea}) is introduced. Because Cl^-, a stable tracer, is less
277 affected by ion exchange, the Cl^- concentration is usually utilized to calculate f_{sea} value through
278 Eq.(12) (Argamasilla et al. 2017; Mountadar et al. 2018).

279 $$f_{sea}=\frac{C_{Cl,\ sample}-C_{Cl,fresh}}{C_{Cl,\ sea}-C_{Cl,fresh}} \quad (12)$$

280 Where $C_{Cl,\ sample}$, $C_{Cl,\ sea}$, and $C_{Cl,\ fresh}$ are the Cl^- concentrations in groundwater sample, seawater,
281 and freshwater, respectively.

282 It is assumed that the groundwater sample having the lowest TDS is freshwater (Han et al.

283 2015). Because of the high solubility of Cl^-, the dissolution of aquifer bedrock and seawater
284 intrusion are its primary source (Argamasilla et al. 2017). Fig. 4(b) showed that the f_{sea} varied
285 with TDS, and the f_{sea} was in the range of 0–6.42%, with a mean of 0.86%, suggesting that
286 moderate seawater intrusion has impacted the shallow groundwater. Besides, TDS was not linear
287 with f_{sea} ($R^2 = 0.71$), which also reflects that the water-rock interaction also controls the
288 groundwater quality (Najib et al., 2016).

289 In addition, the theoretical concentration of ion i ($C_{i,\,mix}$) in the combination of seawater and
290 freshwater can be calculated with f_{sea} value by Eq.(13) (Appelo and Postma 2005).

291 $$C_{i,\,mix}=f_{sea}\times C_{i,\,sea}+\left(1-f_{sea}\right)\times C_{i,\,fresh} \quad (13)$$

292 Where $C_{i,\,sea}$ and $C_{i,\,fresh}$ are the concentrations of ion i in the seawater and freshwater.

293 Br^- in groundwater in coastal regions is mainly from seawater (Zhao et al. 2017), so the
294 accuracy of the f_{sea} can be assessed by comparing the calculated Br^- concentration with its
295 measured concentration. As seen in Fig. 4(c), it can be found that the calculated and measured
296 concentrations of Br^- were approximately distributed around the 1:1 line, indicating that the
297 calculated f_{sea} is reliable. Nevertheless, most points failed to lie on the 1:1 line, which resulted
298 from the effect of seawater and freshwater mixture. In Fig. S5, the relatively high f_{sea} were
299 mainly distributed in the coastal regions and the middle part of the study area. Therefore,
300 seawater intrusion is more severe in these regions. Also, the distribution of f_{sea} was in accordance
301 with that of Cl^- and Na, proving that the high Na and Cl^- levels in the study area result from the

sea. It is noteworthy that the f_{sea} value in the eastern part of Nantong city was even higher than that in the coastal regions. This is because Nantong city is the most densely populated region in the study area, with high water consumption for industry and agriculture; thus, the massive exploitation of shallow groundwater makes this area suffer from the most severe seawater intrusion.

NO_3^- in groundwater mainly comes from agricultural production and domestic sewage. It is expected that the Cl^-/Na and NO_3^-/Na ratios are high in contaminated groundwater (Liu et al. 2021c). Fig. 4(d) shows that agricultural activities did exert an important impact on shallow groundwater quality. In addition, the ratio between Na+K–Cl^- and HCO_3^-+SO_4^{2-}–Ca–Mg is commonly utilized to identify the influence of the cation exchange in groundwater systems (Liu et al. 2021b). The ratios of most water samples were near the 1:1 line, and Na+K–Cl^- was positively correlated with HCO_3^-+SO_4^{2-}–Ca–Mg, as shown in Fig. 4(e), revealing that the cation exchange process significantly affects groundwater hydrochemistry. Thus, the Chlor-alkali index (CAI) calculated by Eqs. (14–15) is used to determine the cation exchange patterns.

$$\text{CAI-1}=\frac{Cl^- - (Na+K)}{Cl^-} \tag{14}$$

$$\text{CAI-2}=\frac{Cl^- - (Na+K)}{HCO_3^- + SO_4^{2-} + CO_3^{2-} + NO_3^-} \tag{15}$$

Based on Fig. 4(f), the CAI-1 and CAI-2 values of most groundwater samples in the study area were less than 0, suggesting that Na on the surface of clay minerals replaces Ca in groundwater. In the west part of the study area, there was a large amount of Ca in the

321 groundwater due to carbonate dissolution. Meanwhile, the aquifer sediments near the shoreline
322 contained a lot of Na because of seawater intrusion. Na in sediment substituted Ca in
323 groundwater during groundwater runoff, resulting in the gradual decrease of Ca concentration
324 along the flow direction. This is also the reason for the distribution of TH value which was high
325 in the west and low in the east (see Fig. 2(b))

326 The sources of trace elements in shallow groundwater can also be obtained by further
327 analyzing the correlations between different ions in the groundwater. In Table S3, Sr showed a
328 significant positive correlation with both Ca and Mg ($r = 0.556$ and 0.586, respectively, $p <$
329 0.01), and its correlation with HCO_3^- ($r = 0.522$, $p < 0.01$) was greater than that with SO_4^{2-} ($r =$
330 0.393, $p < 0.01$), indicating that strontianite dissolution contributes more to Sr concentration than
331 the dissolution of celestite. Also, a significant positive correlation between Na, Br^- and B could
332 be found in Table S3, suggesting that Br^- and B are marine origin. F^- exhibited a remarkable
333 negative correlation with Ca ($r = -0.692$, $p < 0.01$), which demonstrates that fluorite releases F^- in
334 Na – HCO_3 type groundwater during the process of forming calcite precipitates (Jia et al. 2019).
335 Meanwhile, F^- was significantly positively correlated with Na ($r = 0.425$, $p < 0.01$), because the
336 decline of Ca concentration in groundwater, which is due to the cation exchange adsorption
337 between Na in the sediment and Ca in the groundwater, accelerated the fluorite dissolution (Liu
338 et al. 2021a). Fe had a significant positive correlation with Mn ($r = 0.748$, $p < 0.01$), but its
339 correlation with SO_4^{2-} was not significant, which is due to the existence of oolitic Fe-Mn nodules

in the aquifer. Thus, Fe and Mn mainly emanate from the weathering of these Fe-Mn nodules. In addition, As was also positively correlated with Fe and Mn with correlation coefficients of 0.416 and 0.377 ($p<0.01$), respectively. The redox of Fe and Mn strongly influences the geochemical cycling of As in groundwater (Saha and Rahman 2020). In the oxygenated environment, As is adsorbed by the oxides and hydroxides of Fe and Mn; while in the anaerobic environment, the reduction of oxides of Fe and Mn decreases the adsorption sites for As on their surface; at the same time, the As(V) is reduced to As(III) which has weak adsorption, thus promoting the release of As from sediment to groundwater (Duan et al. 2017). Besides, As was apparently negatively correlated with NO_3^- ($r = -0.336$, $p < 0.01$). It has been proposed that the reduction of NO_3^- occurs in the presence of denitrifying bacteria; this process can provide As(V) with enough electrons, accelerating the reduction of As(V) to As(III); thus, more As ions are released into the groundwater (Xie et al. 2018). Ni did not exhibit any significant correlations with other trace elements. Ni is an important raw material for industrial activities, and its improper use can lead to groundwater pollution. The Fig. 3(h) showed the central and southeastern parts of the study area had relatively high Ni levels. Because there are a lot of industrial parks located in these regions and the wastewater discharged from industrial activities may elevate level of Ni.

3.3 Shallow groundwater quality assessment in the study area

3.3.1 For irrigation purposes

359 Yangtze River Delta is one of the major agricultural bases in China. Therefore, shallow
360 groundwater is an important water source for agricultural irrigation. The Na% ranged from
361 12.30% to 81.06%, with an average value of 38.05%; and the SAR varied from 0.53 to 11.96
362 with a mean value of 2.70. According to the Wilcox diagram (see Fig. 5(a)), most groundwater
363 samples were in the good to permissible section (68.85%), while 22.95% of the samples were in
364 the doubtful to unsuitable section and 4.92% of the samples belonged to the unsuitable section,
365 indicating that the groundwater is unsuitable for irrigation in some regions with high Na content.
366 In addition, based on the classification proposed by the U.S. Salinity Laboratory (USSL) (see
367 Fig. 5(b)), the majority of the groundwater samples were located in the C3S1 zone (72.13%). In
368 comparison, 27.87% of the samples were situated in the C4S1, C4S2, C4S3, and C3S2 zones,
369 suggesting that nearly 30% of the shallow groundwater is not suitable for irrigation in the study
370 area. In summary, the Na% and SAR values reveal that shallow groundwater in regions with
371 severe seawater intrusion (e.g., Nantong and Haimeng cities) is unsuitable for irrigation. The
372 people in these places should pay special attention to it in agricultural production.
373
374 *3.3.2 For drinking purposes*
375 Fig. S6 demonstrated *Efs* values, the ratios of measured values of hydrochemical indicators
376 to their corresponding upper limits in the national drinking water standard (GB5749-2006).
377 Among them, the indicators with *Efs* > 1 were TDS, TH, Na, Cl^-, SO_4^{2-}, NO_3^-, F^-, Al, Mn, Fe, Ni,

As, B, Cr and Se, with the exceeding rates of 32.79%, 42.62%, 18.3%, 8.20%, 4.92%, 8.20%, 1.64%, 1.64%, 8.20%, 3.28%, 3.28%, 26.23%, 13.11%, 6.56% and 1.64%, respectively. Se and As had the highest exceedance levels, with maximum *Efs* values of 13.57 and 7.78, respectively. There were only 27.87% of water samples whose indicators all met the standard (GB5749-2006). In addition, WQI values of shallow groundwater varied from 17.42 to 140.20, with an average value of 52.02. According to their WQI values, the percentage of groundwater with excellent, good, medium, and poor quality were 9.8%, 52.5%, 31.1%, and 6.6%, respectively. Thus, most shallow groundwater can be utilized for drinking in the study area. Fig. 6(a) presented the spatial distribution of WQI values in the study area. It could be found that the groundwater samples with excellent and good quality were from the eastern and northern parts of the study area. Besides, groundwater samples with medium and poor quality were sporadically distributed in the central part of the study area like Nantong city, and in the southeastern part of the study area like Qidong city.

The HI values of shallow groundwater in the study area were in the range of 0.264–9.555, with a mean of 1.795. The percentage of groundwater samples with HI > 1 in the study area was 44.3%. Overall, groundwater in some regions may pose a significant non-carcinogenic risk to the health of local residents. Fig. 6(b) showed that the groundwater in the southwestern part of Rugao city, Nantong city, and the northern and southeastern coastal regions of Qidong city had HI>1. Except for Rugao city, the spatial distribution of HI was consistent with that of As (see

397 Fig. 3(f)). Thus, As level is the main factor affecting the HI values.

398 Fig. 7 displayed the non-carcinogenic risks of different trace elements obtained by oral
399 intake and dermal absorption in children. The non-carcinogenic risk of each trace element
400 obtained through dermal absorption was 2 orders of magnitude less than that obtained through
401 the oral intake, and HQ_{dermal} was far less than 1, indicating that oral intake is the main health risk
402 exposure pathway and the non-carcinogenic health risk through dermal absorption is negligible.
403 With the exception of As, the maximum HQ_{oral} value of each trace element was less than 1. The
404 mean and maximum values of HQ_{oral} for As were 1.371 and 9.284, showing significant health
405 risks. The average HI value of each trace element was in the order of As (1.374) > Li (0.217) > B
406 (0.052) > Sr (0.030) > Se (0.020) > Cr (0.019) > Tl (0.019) > Ba (0.013) > Sb (0.011) > others. It
407 is worth noting that the maximum *Efs* value of Se was 13.57, and its maximum HI value was
408 0.973, which is close to the threshold value of the non-carcinogenic health risk. The HI values of
409 Al, Mn, Fe, Ni, and B, which exceeded the national drinking water standard, were low, with
410 maximum values of 0.008, 0.096, 0.035, 0.037, and 0.180, respectively. These trace elements
411 have no significant non-carcinogenic health risks.

412 In Fig. S7, As in shallow groundwater made the greatest contribution to the HI calculations,
413 with a mean value of 54.1% and a maximum value of 97.4%; followed by Li, with a mean value
414 of 24.9% and a maximum value of 74.2%; the average contribution of the remaining elements to
415 total HI was less than 10%. In general, the contribution (mean value) of each element to HI in

shallow groundwater in the study area has the following order: As (54.1%) > Li (24.9%) > B (5.0%) > Tl (4.0%) > Sr (3.5%) > Cr (2.2%) > Sb (1.5%) > Ba (1.4%) > Co (1.0%) > others. Long-term ingestion of high As groundwater will lead to serious diseases such as skin, hematological, and renal diseases (Wu et al. 2020). As should be the focus of attention in drinking water risk management in the study area.

As mentioned above, the results of WQI and HI assessments are broadly consistent. For example, in the north part of the study area, the groundwater had good quality with low WQI and HI values; in contrast, the groundwater quality in the middle and southeast parts was poor with high WQI and HI values. However, some areas had opposite WQI and HI values; for instance, the WQI value was low but the HI value was high in southwest Rugao city. This is because WQI chooses the restrictive indicators such as TDS, TH, pH, etc., in the national drinking water standards for water quality evaluation. However, the HI assessment includes some trace elements such as Sr and Li, which are not restricted in national drinking water standards. Therefore, combining the results from these two assessments provides a more comprehensive understanding of the effects of shallow groundwater quality on health. Taken together, the shallow groundwater in some regions may pose significant health risks to local residents. For example, the shallow groundwater in southwest Rugao city, Nantong city, and parts of Qidong city was no longer suitable as drinking water due to the high As concentration which was a severe threat to the health of local residents. High arsenic groundwater is a current environmental and health

problem worldwide (Podgorski and Berg 2020). Numerous studies on the causes and health risks of high arsenic groundwater have been conducted in the Hetao plain and Jianghan plain in China, while the investigations in the Yangtze River Delta have not been reported (Mao et al. 2018; Zheng et al. 2020). Unlike Hetao plain and Jianghan plain, the Yangtze River Delta is one of the most densely populated areas in China. Thus the health risks associated with high arsenic groundwater require more attention.

Since shallow groundwater is an important water source for irrigation, heavy metals in the water can be enriched through crops. However, in this study, the health risk assessments did not consider the elements from food, resulting in an underestimation of health risk. In addition, the relative sparsity of sampling points could lead to the uncertainty of the spatial distribution of groundwater quality. More detailed research should be carried out in regions with severe seawater intrusion and high As concentrations in the future.

4. Conclusions

In this study, the shallow groundwater in the coastal plain of Yangtze River Delta was sampled and analyzed. On this basis, groundwater quality was evaluated using methods such as WQI and HI. The results showed that the shallow groundwater was slightly alkaline in the study area. The mean values of TDS and TH were 930.74 mg/L and 436.20 mg/L, indicating that the groundwater was moderately hard, hard, and very hard. Na and HCO_3^- had the highest

concentrations in the shallow groundwater. The percentages of groundwater samples with Ca+Mg–HCO_3 type and Ca/Na–HCO_3 type were 44.3% and 47.5%, respectively. Sr, Br, F and B were the major trace elements with mean values of 0.4975 mg/L, 0.3729 mg/, 0.3470 mg/L and 0.2888 mg/L, respectively. Meanwhile, As had a relatively high concentration in shallow groundwater (its average value was 0.0115 mg/L). Factors like rock weathering (silicate), cation exchange, seawater intrusion, and industrial and agricultural activities played an important role in the chemical composition of shallow groundwater in the Yangtze River Delta plain. The massive exploitation of shallow groundwater has caused the most severe seawater intrusion in Nantong city. The trace element like Br^- and B in shallow groundwater had a marine origin. Fe and Mn mainly derived from the weathering of Fe–Mn nodules in the sediments; and As was strongly affected by the redox of Fe, Mn, and NO_3^-. In addition, wastewater discharged from industrial activities has contributed to the increased concentration of heavy metals in groundwater. According to the water quality assessment, shallow groundwater in some regions was unsuitable for irrigation. At the same time, TDS, TH, Na, Cl^-, SO_4^{2-}, NO_3^-, F^-, Al, Mn, Fe, Ni, As, B, Cr and Se in some groundwater samples exceeded their corresponding upper limits in the national drinking water standard. There were only 27.87% of the groundwater samples whose indicators were in line with the national drinking water standard. According to the classification of WQI values, excellent, good, medium, poor groundwater samples accounted for 9.8%, 52.5%, 31.1%, and 6.6%, respectively. The analysis of health risk showed that 44.3% of the water

samples had significant health risks, and As played the most important role in health risk, with a mean contribution of 54.1% to the total HI; therefore, As should become the focus in drinking water management in the study area. The shallow groundwater quality in the Yangtze River Delta, especially the concentrations of trace elements and their health risk assessment, has been neglected for a long time. It is necessary to conduct long-term monitoring of As contamination in the Yangtze River Delta and to take measures to prevent and control groundwater contamination. In the meantime, new high-quality water sources should be sought for the regions, such as Nantong city, where seawater intrusion is serious; and shallow groundwater extraction should be reduced to maintain sustainable groundwater resource management.

Ethics approval and consent to participate

Not applicable.

Consent for publication

Not applicable.

Author Contributions

Taotao Lu: Conceptualization, Methodology, Investigation, Writing- Original draft preparation; Runzhe Li: Methodology, Investigation; Aira Sacha Nadine Ferrer: Resources;

Shuang Xiong: Software, Investigation; Pengfei Zou: Supervision, Funding acquisition; Hao Peng: Formal analysis, Writing- Original draft preparation, Writing- Reviewing and Editing.

Funding

This project was supported by New Era Health Industry (Group) Co. Ltd. (ZAT2019X01002) and the China Scholarship Council (201708420145).

Conpeting Interests

The authors declare that they have no known competing financial interests or personal relationships that could have appeared to influence the work reported in this paper.

Availability of data and materials

Supplementary Material data to this article can be found in the online version of this article.

References

Appelo CAJ, Postma D (2005) Geochemistry, Groundwater and Pollution, second ed. A.A. Balkema Publishers, Leiden

Argamasilla M, Barberá J, Andreo B (2017) Factors controlling groundwater salinization and hydrogeochemical processes in coastal aquifers from southern Spain. Sci Total Environ

580:50–68

Cao T, Han D, Song X, Trolle D (2020) Subsurface hydrological processes and groundwater residence time in a coastal alluvium aquifer: Evidence from environmental tracers (δ18O, δ2H, CFCs, 3H) combined with hydrochemistry. Sci Total Environ 743:140684

Chen L, Ma T, Wang Y, Zheng J (2020) Health risks associated with multiple metal (loid) s in groundwater: A case study at Hetao Plain, northern China. Environ Pollut 263:114562

Duan Y, Gan Y, Wang Y, Liu C, Yu K, Deng Y, Zhao K, Dong C (2017) Arsenic speciation in aquifer sediment under varying groundwater regime and redox conditions at Jianghan Plain of Central China. Sci Total Environ 607:992–1000

Gao Y, Qian H, Ren W, Wang H, Liu F, Yang F (2020) Hydrogeochemical characterization and quality assessment of groundwater based on integrated-weight water quality index in a concentrated urban area. J Clean Prod 260:121006

Gibbs RJ (1970) Mechanisms controlling world water chemistry. Science 170:1088–1090

Han D, Post VE, Song X (2015) Groundwater salinization processes and reversibility of seawater intrusion in coastal carbonate aquifers. J Hydrol 531:1067–1080

Hao C, Zhang W, Gui H (2020) Hydrogeochemistry characteristic contrasts between low-and high-antimony in shallow drinkable groundwater at the largest antimony mine in Hunan province, China. Appl Geochem 117:104584

Hou Q, Zhang Q, Huang G, Liu C, Zhang Y (2020) Elevated manganese concentrations in

shallow groundwater of various aquifers in a rapidly urbanized delta, south China. Sci Total Environ 701:134777

Islam ARMT, Al Mamun A, Rahman MM, Zahid A (2020) Simultaneous comparison of modified-integrated water quality and entropy weighted indices: implication for safe drinking water in the coastal region of Bangladesh. Ecol Indic 113:106229

Jia H, Qian H, Qu W, Zheng L, Feng W, Ren W (2019) Fluoride occurrence and human health risk in drinking water wells from southern edge of Chinese Loess Plateau. Int J Environ Res Public Health 16:1683

Li Q, Zhang Y, Chen W, Yu S (2018) The integrated impacts of natural processes and human activities on groundwater salinization in the coastal aquifers of Beihai, southern China. Hydrogeol J 26:1513–1526

Li X, Tang C, Cao Y, Li D (2020) A multiple isotope (H, O, N, C and S) approach to elucidate the hydrochemical evolution of shallow groundwater in a rapidly urbanized area of the Pearl River Delta, China. Sci Total Environ 724:137930

Lima IQ, Ramos OR, Munoz MO, Aguirre JQ, Duwig C, Maity JP, Sracek O, Bhattacharya P (2020) Spatial dependency of arsenic, antimony, boron and other trace elements in the shallow groundwater systems of the Lower Katari Basin, Bolivian Altiplano. Sci Total Environ 719:137505

Liu J, Peng Y, Li C, Gao Z, Chen S (2021a) A characterization of groundwater fluoride,

549 influencing factors and risk to human health in the southwest plain of Shandong Province,
550 North China. Ecotoxicol Environ Saf 207:111512
551 Liu J, Peng Y, Li C, Gao Z, Chen S (2021b) Characterization of the hydrochemistry of water
552 resources of the Weibei Plain, Northern China, as well as an assessment of the risk of high
553 groundwater nitrate levels to human health. Environ Pollut 268:115947
554 Liu J, Peng Y, Li C, Gao Z, Chen S (2021c) An investigation into the hydrochemistry, quality and
555 risk to human health of groundwater in the central region of Shandong Province, North
556 China. J Clean Prod 282:125416
557 Liu, X., Wang, X., Zhang, L., Fan, W., Yang, C., Li, E., Wang, Z., 2021d. Impact of land use on
558 shallow groundwater quality characteristics associated with human health risks in a typical
559 agricultural area in Central China. Environ. Sci. Pollut. Res. 28, 1712–1724
560 Long, J., Luo, K., 2020. Elements in surface and well water from the central North China Plain:
561 enrichment patterns, origins, and health risk assessment. Environ. Pollut. 258, 113725
562 Long X, Liu F, Zhou X, Pi J, Yin W, Li F, Huang S, Ma F (2021) Estimation of spatial
563 distribution and health risk by arsenic and heavy metals in shallow groundwater around
564 Dongting Lake plain using GIS mapping. Chemosphere 269:128698
565 Ma Q, Luo Z, Howard KW, Wang Q (2018) Evaluation of optimal aquifer yield in Nantong City,
566 China, under land subsidence constraints. Q J Eng Geol Hydrogeol 51:124–137
567 Mao C, Tan H, Song Y, Rao W (2020) Evolution of groundwater chemistry in coastal aquifers of

568 the Jiangsu, east China: Insights from a multi-isotope (δ2H, δ18O, 87Sr/86Sr, and δ11B)
569 approach. J Contam Hydrol 235:103730
570 Mao R, Guo H, Xiu W, Yang Y, Huang X, Zhou Y, Li X, Jin J (2018) Characteristics and
571 compound-specific carbon isotope compositions of sedimentary lipids in high arsenic
572 aquifers in the Hetao basin, Inner Mongolia. Environ Pollut 241:85–95
573 Mountadar S, Younsi A, Hayani A, Siniti M, Tahiri S (2018) Groundwater salinization process in
574 the coastal aquifer sidi abed-ouled ghanem (province of el Jadida, Morocco). J African
575 Earth Sci 147:169–177
576 Najib S, Fadili A, Mehdi K, Riss J, Makan A, Guessir H (2016) Salinization process and coastal
577 groundwater quality in Chaouia, Morocco. J African Earth Sci 115:17–31
578 Narayanamoorthy S, Annapoorani V, Kang D, Baleanu D, Jeon J, Kureethara JV, Ramya L
579 (2020) A novel assessment of bio-medical waste disposal methods using integrating
580 weighting approach and hesitant fuzzy MOOSRA. J Clean Prod 275:122587
581 Peng H, Yao F, Xiong S, Wu Z, Niu G, Lu T (2021a) Strontium in public drinking water and
582 associated public health risks in Chinese cities. Environ Sci Pollut Res 28:23048–23059
583 Peng H, Zou P, Ma C, Xiong S, Lu T (2021b) Elements in potable groundwater in Rugao
584 longevity area, China: Hydrogeochemical characteristics, enrichment patterns and health
585 assessments. Ecotoxicol Environ Saf 218:112279
586 Podgorski J, Berg M (2020) Global threat of arsenic in groundwater. Science 368:845–850.

587 Saha N, Rahman MS (2020) Groundwater hydrogeochemistry and probabilistic health risk
588 assessment through exposure to arsenic-contaminated groundwater of Meghna floodplain,
589 central-east Bangladesh. Ecotoxicol Environ Saf 206:111349
590 Samsudin AR, Haryono A, Hamzah U, Rafek A (2008) Salinity mapping of coastal groundwater
591 aquifers using hydrogeochemical and geophysical methods: a case study from north
592 Kelantan, Malaysia. Environ Geol 55:1737–1743
593 Selinus O, Alloway B, Centeno JA, Finkelman RB, Fuge R, Lindh U, Smedley P (2016)
594 Essentials of medical geology. Springer, Dordrecht
595 Wang L, Yin Z, Jing C (2020) Metagenomic insights into microbial arsenic metabolism in
596 shallow groundwater of Datong basin, China. Chemosphere 245:125603
597 Wu C, Fang C, Wu X, Zhu G (2020) Health-Risk Assessment of Arsenic and Groundwater
598 Quality Classification Using Random Forest in the Yanchi Region of Northwest China.
599 Expos Health 12:761–774
600 Wu C, Luo Y, Gui T, Yan S (2014) Characteristics and potential health hazards of organochlorine
601 pesticides in shallow groundwater of two cities in the Yangtze River Delta. Clean–Soil Air
602 Water 42:923–931
603 Wu J, Sun Z (2016) Evaluation of shallow groundwater contamination and associated human
604 health risk in an alluvial plain impacted by agricultural and industrial activities, mid-west
605 China. Expos Health 8:311–329

606 Xie Z, Wang J, Wei X, Li F, Chen M, Wang J, Gao B (2018) Interactions between arsenic
607 adsorption/desorption and indigenous bacterial activity in shallow high arsenic aquifer
608 sediments from the Jianghan Plain, Central China. Sci Total Environ 644:382–388
609 Zhang Q, Qian H, Xu P, Hou K, Yang F (2021) Groundwater quality assessment using a new
610 integrated-weight water quality index (IWQI) and driver analysis in the Jiaokou Irrigation
611 District, China. Ecotoxicol Environ Saf 212:111992
612 Zhang Q, Xu P, Qian H (2020) Groundwater quality assessment using improved water quality
613 index (WQI) and human health risk (HHR) evaluation in a semi-arid region of northwest
614 China. Expos Health 12:487–500
615 Zhao Q, Su X, Kang B, Zhang Y, Wu X, Liu M (2017) A hydrogeochemistry and multi-isotope
616 (Sr, O, H, and C) study of groundwater salinity origin and hydrogeochemcial processes in
617 the shallow confined aquifer of northern Yangtze River downstream coastal plain, China.
618 Appl Geochem 86:49–58
619 Zheng T, Deng Y, Wang Y, Jiang H, Xie X, Gan Y (2020) Microbial sulfate reduction facilitates
620 seasonal variation of arsenic concentration in groundwater of Jianghan Plain, Central China.
621 Sci Total Environ 735:139327
622 Zhi C, Cao W, Zhang Z, Li Z, Ren Y (2021) Hydrogeochemical characteristics and processes of
623 shallow groundwater in the Yellow River Delta, China. Water 13:534
624

625 **Table 1.** Chemical composition and their statistical characteristics in the shallow groundwater in

626 the study area

Unit	Project	Detection Limit	Minimum value	Maximum value	Average value	Median	Standard deviation	Shapiro-Wilk Test	
								H-value	Sig
--	pH	--	6.90	7.90	7.31	7.30	0.23	0.967	0.104
mg/L	TDS	--	411.45	2361.77	930.74	841.68	370.26	0.907	0
mg/L	TH	--	181.63	897.74	436.20	418.98	144.02	0.959	0.041
mg/L	Na	0.002	24.00	482.79	124.08	99.90	92.52	0.828	0
mg/L	Mg	0.01	20.11	106.15	52.21	48.96	19.73	0.961	0.047
mg/L	K	0.001	2.61	221.00	22.80	11.93	31.75	0.517	0
mg/L	Ca	0.02	22.46	277.49	87.46	81.55	45.27	0.905	0
mg/L	HCO_3^-	0.01	292.47	860.20	543.87	504.65	135.43	0.944	0.008
mg/L	Cl^-	0.004	11.18	806.00	117.99	88.20	114.16	0.648	0
mg/L	NO_3^-	0.0006	0.03	139.77	32.29	22.90	32.34	0.854	0
mg/L	SO_4^{2-}	0.002	6.57	271.90	96.12	87.79	63.07	0.906	0
mg/L	F^-	0.00002	0.0240	1.0790	0.3470	0.2977	0.2103	0.867	0
mg/L	Br^-	0.00002	0.0000	2.6350	0.3729	0.2598	0.4114	0.215	0
mg/L	Sr	0.0001	0.1814	0.9882	0.4975	0.4532	0.1800	0.958	0.037
mg/L	Al	0.00004	0.0007	0.2291	0.0526	0.0410	0.0443	0.840	0
mg/L	Cr	0.00005	0.0000	0.0104	0.0014	0.0006	0.0020	0.606	0
mg/L	Mn	0.00002	0.0000	0.3732	0.0204	0.0021	0.0588	0.388	0
mg/L	Fe	0.00006	0.0017	0.6774	0.0484	0.0224	0.1032	0.345	0
mg/L	Ni	0.00002	0.0000	0.0205	0.0014	0.0007	0.0036	0.306	0
mg/L	Cu	0.00002	0.0000	0.0736	0.0030	0.0015	0.0094	0.229	0
mg/L	Zn	0.00004	0.0009	0.5300	0.0339	0.0144	0.0787	0.358	0
mg/L	As	0.00002	0.0000	0.0778	0.0115	0.0037	0.0179	0.653	0
mg/L	Li	0.00006	0.0021	0.0366	0.0121	0.0121	0.0077	0.938	0.004
mg/L	B	0.00004	0.0285	1.0065	0.2888	0.2030	0.21901	0.789	0
mg/L	Se	0.00004	0.0000	0.1357	0.0027	0.0000	0.0173	0.184	0
mg/L	Mo	0.00002	0.0000	0.0076	0.0011	0.0006	0.0014	0.746	0
mg/L	Ba	0.00002	0.0074	0.2828	0.0685	0.0604	0.0397	0.628	0
μg/L	Ag	0.002	0.02	0.03	0.02	0.02	0.00	0.500	0
μg/L	Cd	0.004	0.00	0.06	0.03	0.03	0.02	0.837	0
μg/L	Sn	0.002	0.00	0.10	0.01	0.00	0.02	0.477	0
μg/L	Sb	0.002	0.00	1.70	0.10	0.07	0.22	0.331	0
μg/L	W	0.01	0.00	1.27	0.09	0.04	0.17	0.366	0
μg/L	Tl	0.005	0.00	0.02	0.00	0.00	0.01	0.659	0
μg/L	Pb	0.002	0.00	0.92	0.04	0.01	0.14	0.286	0
μg/L	Be	0.006	0.00	1.40	0.10	0.00	0.23	0.510	0
μg/L	Co	0.002	0.00	0.30	0.08	0.06	0.06	0.789	0

Note: The concentration of 0.0000 mg/L or 0.00 μg/L means below the detection line. -- represents not applicable

627

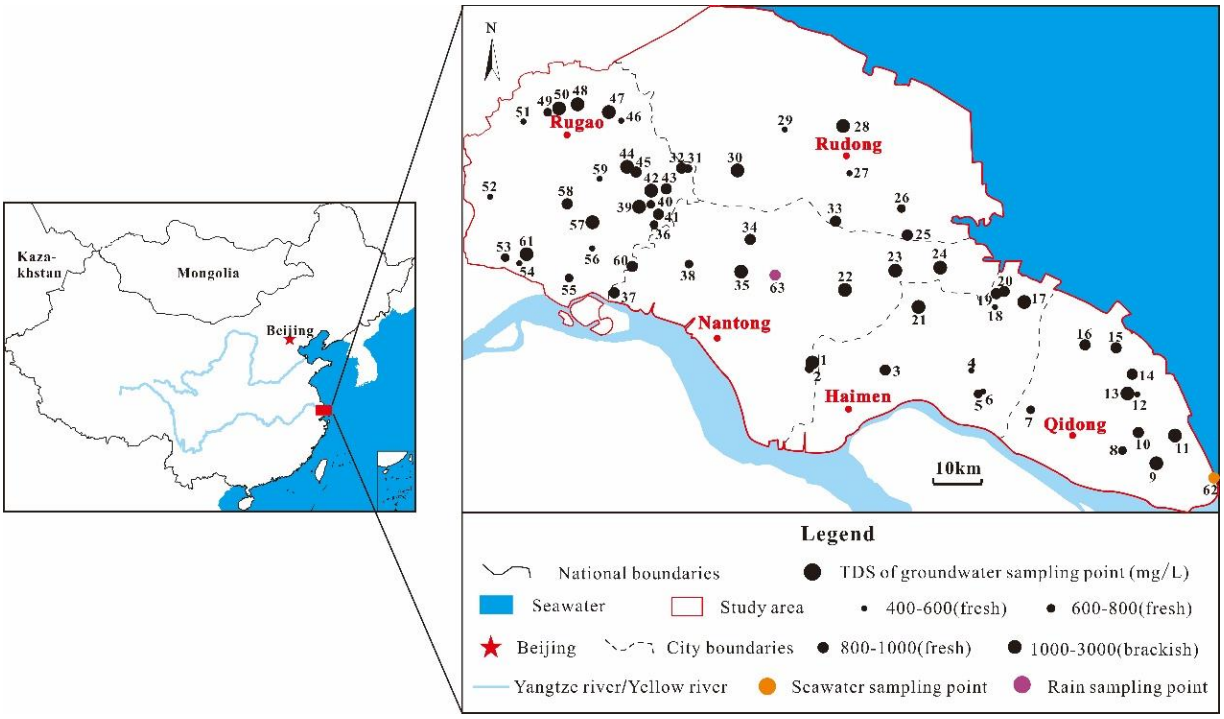

628

629 **Fig. 1** Spatial distribution of groundwater samples in the study area.

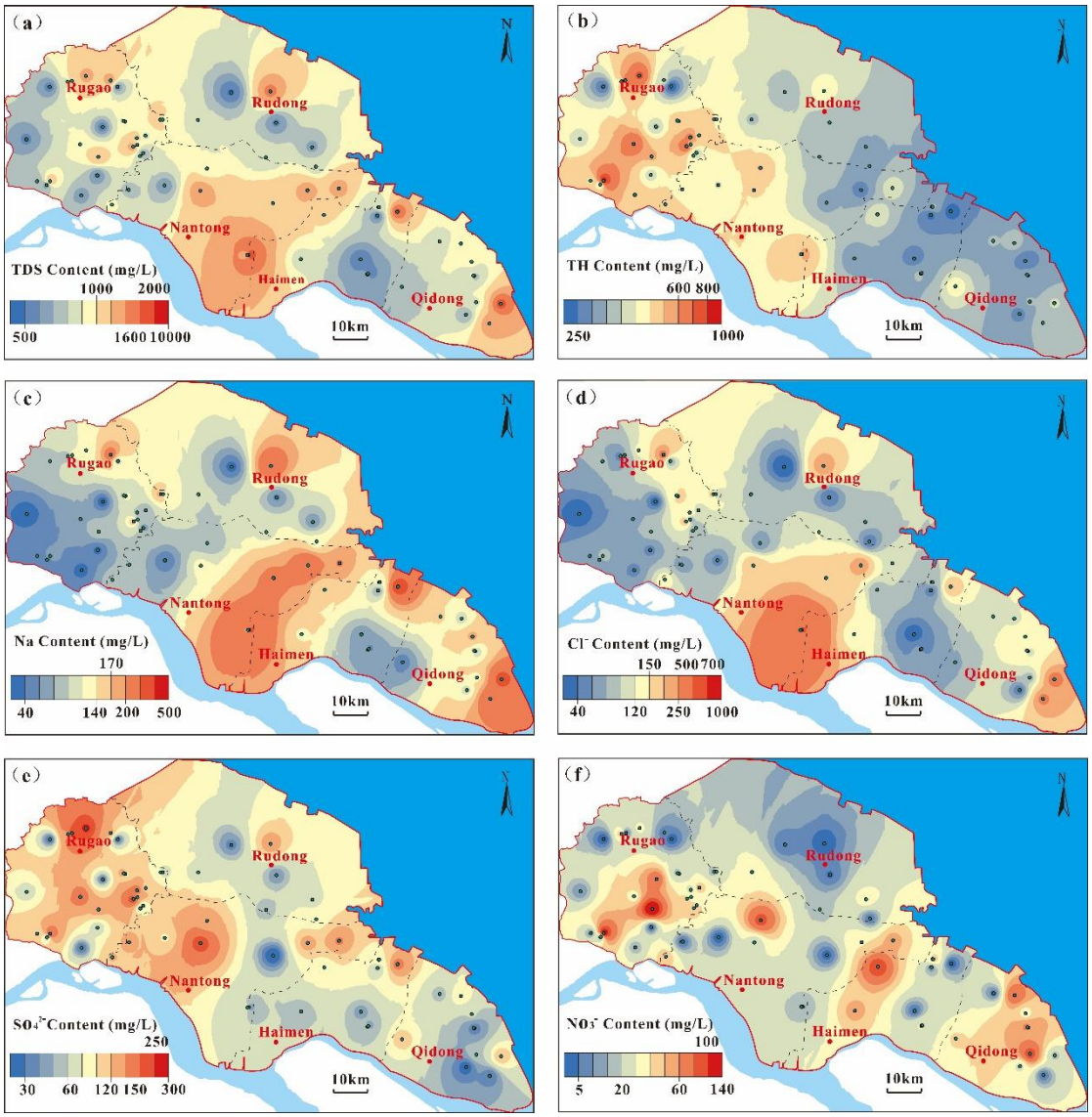

630

631 **Fig. 2** The spatial distributions of the main components in shallow groundwater in the study area:

632 (a) TDS, (b) TH, (c) Na, (d) Cl^-, (e) SO_4^{2-} and (f) NO_3^-.

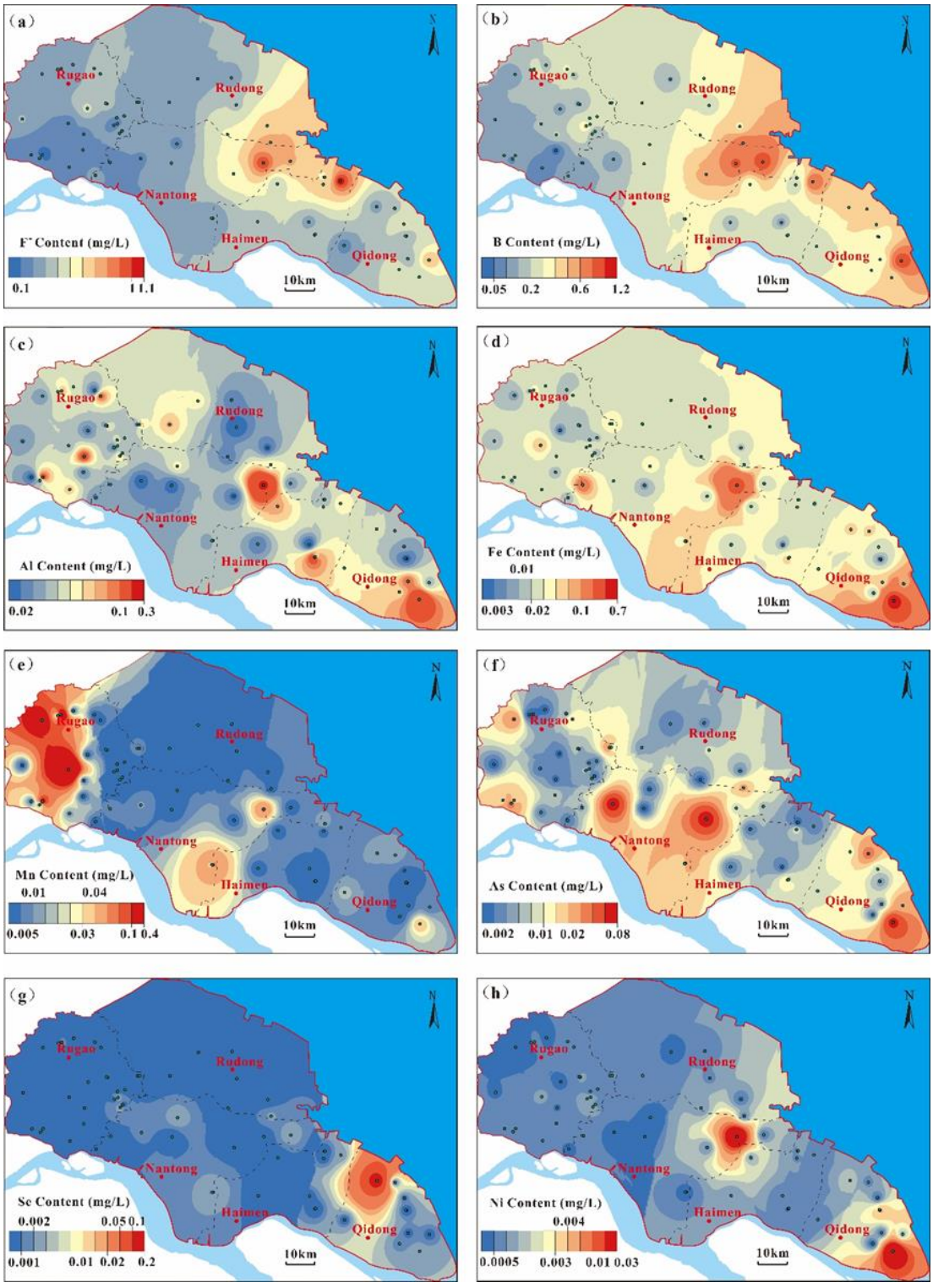

633

634 **Fig. 3** The spatial distributions of the trace elements in shallow groundwater in the study area:

635 (a) F^-, (b) B, (c) Al, (d) Fe, (e) Mn, (f) As, (g) Se, and (h) Ni.

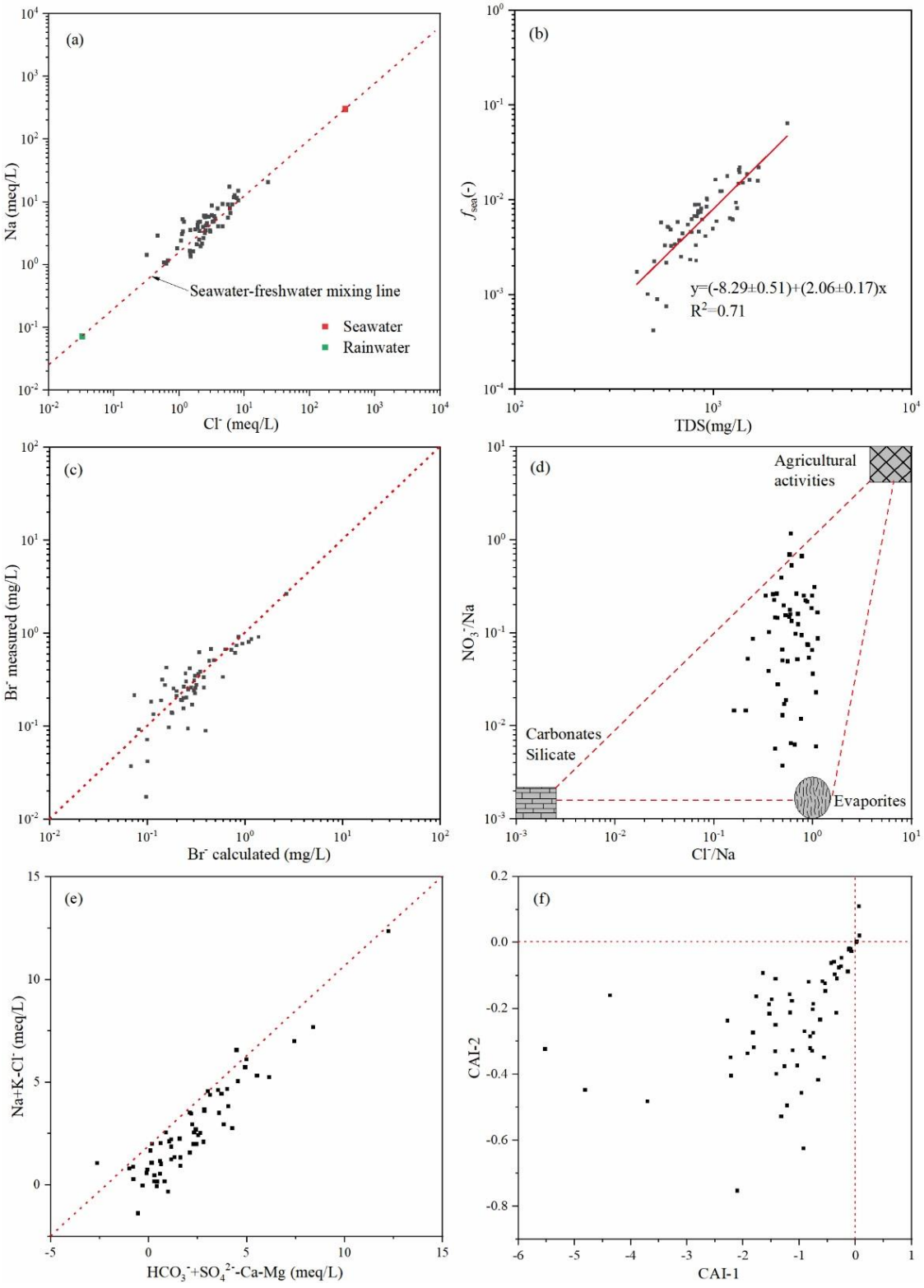

636

637 **Fig. 4** Ratio graphs of different indicators in shallow groundwater in the study area.

638

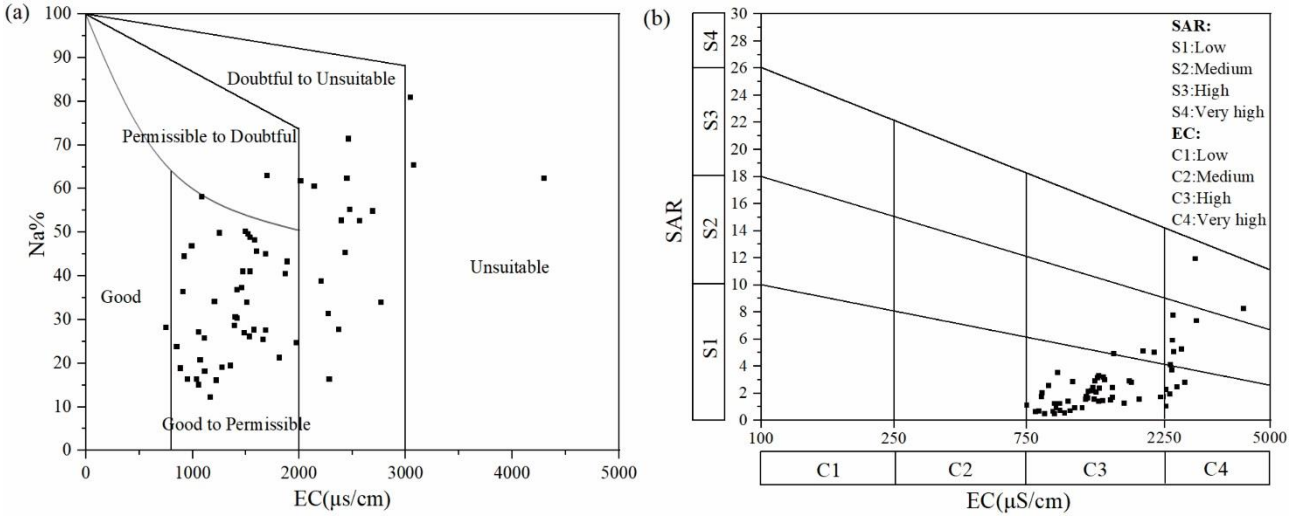

639

640 **Fig. 5** Wilcox diagram (a) and USSL diagram (b) for the assessment of the shallow groundwater

641 quality for irrigation in the study area.

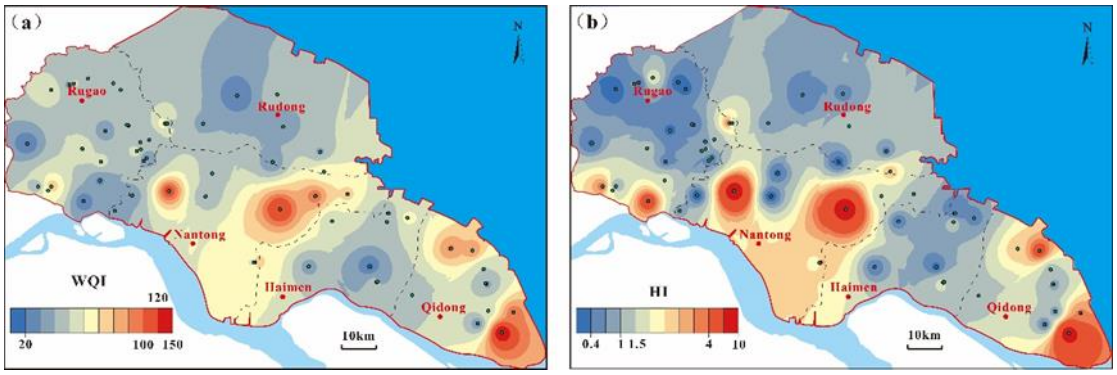

642

643 **Fig. 6** The spatial distribution of WQI value (a) and HI value (b) in the study area.

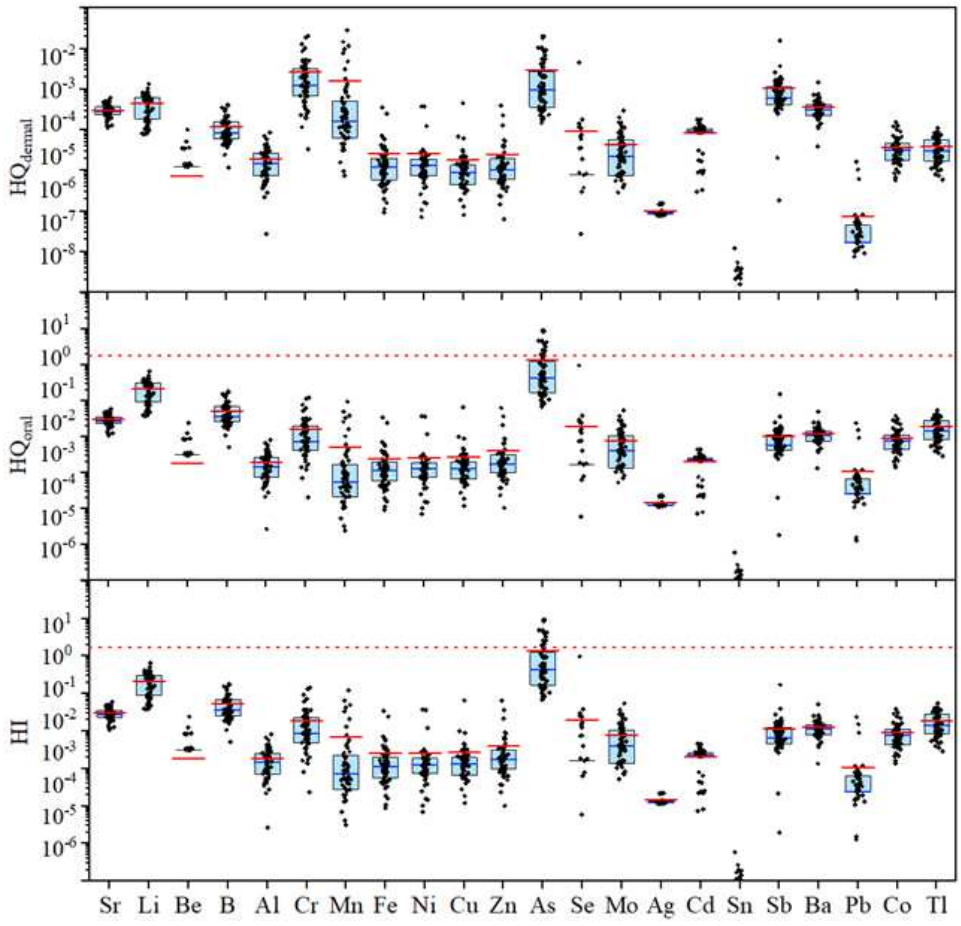

644

645 **Fig. 7** Non-carcinogenic risks in children from different exposure routes (dermal absorption and

646 oral ingestion).

Supplementary Files

This is a list of supplementary files associated with this preprint. Click to download.

- LuetalSupplementaryMaterialfinal.docx